ELSEVIER

Biophysical Chemistry 50 (1994) 293–304

Biophysical Chemistry

Use of nonradiative decays of extrinsic fluorophores as structural and dynamical probes in protein environments: fluorescence quenching

Cristiano Viappiani [1]

Department of Physics, University of Parma Viale delle Scienze, 43100 Parma, Italy

(Received 26 July 1993; accepted in revised version 17 November 1993)

Abstract

In this work a combined pulsed-laser, time-resolved photoacoustic calorimetry (PAC) and fluorescence study is presented on two widely used covalent protein probes, fluorescein-5-isothiocyanate (FITC) and 6-acryloyl-2-dimethylaminonaphtalene (acrylodan). Three proteins that contain a single free thiol, namely carbonic anhydrase, bovine serum albumin (BSA) and papain, have been selectively labelled with FITC and acrylodan, and their fluorescence emission was quenched with KI. Nonradiative decays of the excited states of FITC are used to complement the information usually obtained by monitoring the quenching of fluorescence emission. Data analysis evidences the dependence of the nonradiative quenching constants on the exposure of the dye to the solvent, and shows the involvement of a triplet state of FITC in the non radiative deexcitation. The shielding of the binding sites from the solvent is demonstrated also by the fluorescence emission of acrylodan and by the Stern–Volmer analysis of fluorescence quenching by KI. From photoacoustic data, an estimate of the fluorescent quantum yield of bound FITC is obtained. This work demonstrates the complete equivalence of quenching data obtained by fluorescence and photoacoustics measurements and shows that this combined approach allows a better control of the photophysics of the dyes involved in the quenching process.

Key words: Photoacoustics; Nonradiative decays; Fluorescence quenching; Fluorescence probes

1. Introduction

The usage of extrinsic fluorescent probes to study the dynamics and the structure of macromolecules has become very popular in the past years, due to the possibility of monitoring various physical–chemical parameters, such as environment polarity, pH and viscosity [1]. Site-specific probes have been developed to test both the surrounding of the site and the accessibility to external molecules and by means of the dynamic properties of these dyes, some hints on the local macromolecular dynamics have been obtained. The values of the fluorescent quantum yield and of the maximum emission wavelength of a protein bound fluorophore can give some information concerning local physical–chemical parameters,

[1] Fax: 39-521-905223.

SSDI 0301-4622(93)E0097-0

such as polarity and pH, while excited state lifetimes are sensors of local and/or global movements of the macromolecule.

Protein fluorescence quenching of both amino acid side chains and bound probes has become a widely used technique in protein biophysics and has allowed the determination of both structural and dynamic properties of microenvironments inside the macromolecule [2–5]. Determination of quenching parameters allows the estimation of the exposure degree of the molecule to the solvent [6]. Due to the high sensitivity of the technique and the relative ease by which quenching experiments are performed, the method has become quite a useful tool for the protein biophysicist.

Pulsed-laser, time-resolved photoacoustic calorimetry (PAC) is a technique that provides information on nonradiative deactivation channels of molecular excited states [7]. In a typical experiment, the heat emitted by a photoexcited sample induces pressure waves in the solution, which are detected by an ultrasonic transducer. By comparing the photoacoustic (PA) waveform of the sample with the waveform obtained by a calorimetric standard, which is a chromophore that releases all the absorbed energy as heat within a few ns, it is possible to determine the fraction of absorbed energy released by the sample as heat. PA is related to absorption and complementary to luminescence, since it requires absorption of a photon, but then detects the fraction of the photon energy released as heat, rather than as light.

The complementarity of photoacoustic and fluorescence measurements has been stressed several times in the past years. The PA determination of fluorescent quantum yields has been shown to be possible and the accuracy to be more than satisfactory [8–10].

In recent years some quenching studies have been performed on organic dyes by means of PA techniques on fluorescent singlet states [11] and on triplet states [12,13], yielding interesting results. The gain in experimental resolution achieved with real-time deconvolution analysis of PA waveforms [14,15] has allowed fairly accurate analysis of collisional fluorescence quenching by KI on several organic dyes [12,13,16]. Quenching experiments performed on fluorescent dyes in ethanol solutions [16] showed a good accordance between fluorescence and PA data. The two processes can effectively be regarded as complementary to each other, since the quenching constants recovered from the two techniques are identical and the fluorescence quantum yield, as determined by the fitting of PA data, is in accordance with literature data. However, in the case of 9,10-dichloroanthracene, where highly efficient intersystem crossing is known to occur, no satisfactory explanation of the quenching process was given. Unlike the other cases, a simple model based on generally valid energy balance considerations is not accurate enough to describe the quenching process in this system, for which a more precise rationalization of the photophysics and the photochemistry would probably better account for the observed data trend. A general conclusion that can be drawn from these results is that this combined fluorescence and PA approach to study fluorescence quenching processes gives a better understanding of the fate of absorbed energy within a fluorophore. It seems therefore promising to extend this methodology to the investigation of systems of biological interest, such as fluorescent protein probes, for which an increased control on the primary photophysical events may help understanding the quenching results. As a test of the methodology, two commonly used fluorescent protein dyes have been used in quenching experiments.

Fluorescein-5-isothiocyanate (FITC) is a widely used covalent protein probe [1,17–20]. At neutral pH, the absorption peak of the lowest energy transition is located at 493 nm, with no overlap with the bands of the aromatic residues of proteins. Upon changing the pH, the peaks undergo changes in relative intensity, whereas no emission shifts are evident from the spectra. The value of the fluorescent quantum yield is ≈ 0.7 at pH 7. The probe is thiol selective at neutral pH, while at higher values it also reacts with the amino group of lysines.

6-acryloyl-2-dimethylaminonaphtalene (acrylodan) is a thiol selective protein probe. The fluorescent quantum yield of this probe is markedly enhanced after reaction with thiols and these

adducts are very sensitive to dipolar perturbation from their environment [21]. Both absorption and fluorescence are affected by environment polarity [22] with very large shifts in peak positions and changes in relative intensity. The excitation peak of acrylodan fluorescence is located around 360 nm, the exact wavelength depending on the solvent, way out from the aromatic bands of proteins. These features make the probe very useful in the study of hydrophobic pockets, conformational changes and dielectric relaxation processes in proteins.

The photoacoustics of FITC and acrylodan, free and conjugated to some proteins, was investigated in order to test the reliability of the nonradiative decays of the fluorophore as probe of the macromolecular structure and dynamics. Three proteins that contain a single free thiol, carbonic anhydrase, bovine serum albumin (BSA) and papain, have been selectively labelled with FITC and acrylodan, and their fluorescence emission was quenched with KI. Carbonic anhydrase and papain are known from previous studies to have an hydrophobic pocket surrounding the free thiol [21], the one on papain being located at the active site of the enzyme. BSA has too a single free thiol [23], whose location is possibly shielded from the solvent.

The calculations outlined in the next section give a description of the quenching process and are based on the conservation of energy [7], expressed as the balance of the input energy to the sum of the different forms of output energy. Fluorescence and PA data are used as complementary and independent tools to monitor the physical process under investigation.

2. Model

In this section, some previously obtained results are summarized; the reader may refer to ref. [16] for a more detailed description of the derivation of the various expressions. A list of symbols can be found in Table 1.

An important general remark, about time resolution of pulsed PAC needs to be done at this point. Heat release events occurring in time scales much shorter than the typical instrumental resolution which is ≈ 50 ns for a 32 MS/s digital scope and 1 MHz piezoelectric transducer as in our instrumentation, are integrated by the transducer. It is not possible to have any information on their time scale, apart from the fact that they are fast [15,24]. Amplitude values are nevertheless obtainable, and this fraction of absorbed energy released as heat in less than a few nanoseconds is usually called prompt heat and indicated as α. Events occurring on time scales longer than 5 μs are ignored by the transducer and cannot be detected. In the intermediate range, real-time deconvolution of photoacoustic

Table 1
List of symbols used throughout the paper

Parameter	Definition
E	incident light molar energy content ($h\nu_{ex}$) (kcal/mol)
E_T	triplet state energy (kcal/mol)
ν_{em}	average fluorescence frequency (Hz)
τ	fluorescence lifetime (s)
$(\Phi_{FM})_0$	fluorescent quantum yield in the absence of the quencher
(Φ_{FM})	fluorescent quantum yield in the presence of the quencher
α	fraction of prompt heat
α_1	fraction of prompt heat in the presence of a second, resolvable, decay
α_2	fraction of heat emitted in the second, slower, decay
$(\Phi_{TM})_0$	intersystem crossing quantum yield in the absence of the quencher
(Φ_{TM})	intersystem crossing quantum yield in the presence of the quencher
q_{PT}	phosphorescence quantum efficiency
k_{QM}	bimolecular quenching constant (s^{-1} M^{-1})

waveforms yields preexponential factors, α_i, that express the fractions of absorbed light energy converted into heat by nonradiative processes, and the average lifetimes τ_i of each process. A certain amount of prompt heat will always be present in the photoacoustic signal due to the very efficient vibrational relaxation. The fractional amplitude of this decay is usually referred to as α_1, and the corresponding lifetime τ_1 is conventionally indicated as shorter than 1 ns.

In the following a model fluorophore is considered, which undergoes intersystem crossing to a triplet state T_1 laying below the first excited singlet S_1, but not showing any photochemistry.

Fluorescence quenching by a collisional quencher Q is properly described by the Stern–Volmer equation [25,26]. The ratio of the fluorescent quantum yield in the presence and in the absence of the quencher, is given by

$$\frac{\Phi_{FM}}{(\Phi_{FM})_0} = \frac{1}{1+\tau k_{QM}[Q]}, \tag{1}$$

where τ is the fluorescence lifetime of S_1, k_{QM} is the bimolecular rate constant and [Q] is the quencher concentration; τk_{QM} is often referred to as the quenching constant of the process, K.

Since singlet lifetimes are generally of the order of nanoseconds, no other heat than prompt heat is expected in the absence of intersystem crossing, and α can be written as [9]

$$\alpha = 1 - (\Phi_{FM})_0 \frac{\nu_{em}}{\nu_{ex}}, \tag{2}$$

ν_{ex} and ν_{em} being the exciting light and average fluorescence emission frequency respectively. In the presence of a collisional quencher Q the expression for α is readily obtained by sustituting Eq. (1) into Eq. (2),

$$\alpha = 1 - \Phi_{FM}\frac{\nu_{em}}{\nu_{ex}} = \frac{1+\tau k_{QM}[Q] - (\Phi_{FM})_0\frac{\nu_{em}}{\nu_{ex}}}{1+\tau k_{QM}[Q]}. \tag{3}$$

When intersystem crossing is not negligible, a second decay may be detected by the PA instrument, originating from the triplet state deexcitation, and the amplitudes of the two decays can be written as

$$\alpha_1 = 1 - (\Phi_{FM})_0\frac{\nu_{em}}{\nu_{ex}} - (\Phi_{TM})_0\frac{E_T}{E}, \tag{4}$$

$$\alpha_2 = (\Phi_{TM})_0(1-q_{PT})\frac{E_T}{E}. \tag{5}$$

As previously stated, the possibility of reactions from the triplet state is neglected in this calculation. The detection of a second component is obviously possible only if its lifetime falls within the resolution range of the instrument. If its lifetime is shorter than about 50 ns it is detected as prompt heat, whereas if it is longer than 5 μs it is not detectable at all. It is necessary to point out that if the lifetime of the slow decay is long enough to be undetectable, the above formalism is still valid, whereas if the triplet lifetime is shorter than 50 ns, the energy balance becomes more complicated because of the mixing of the two different heat sources.

The presence of a collisional heavy atom quencher may result in an increased probability for intersystem crossing. The ratio $\Phi_{FM}/(\Phi_{FM})_0$ is again given by Eq. (1) whereas the intersystem crossing quantum yield Φ_{TM} becomes [27]

$$\Phi_{TM} = \frac{(\Phi_{TM})_0 + \tau k_{QM}[Q]}{1+\tau k_{QM}[Q]}. \tag{6}$$

The corresponding expressions for the non radiative preexponentials are obtained by substituting Eq. (6) into Eqs. (3) and (4):

$$\alpha_1 = 1 - \frac{(\Phi_{FM})_0\frac{\nu_{em}}{\nu_{ex}}}{1+\tau k_{QM}[Q]} - \frac{(\Phi_{TM})_0 + \tau k_{QM}[Q]}{1+\tau k_{QM}[Q]}\frac{E_T}{E}, \tag{7}$$

$$\alpha_2 = (1-q_{PT})\frac{(\Phi_{TM})_0 + \tau k_{QM}[Q]}{1+\tau k_{QM}[Q]}\frac{E_T}{E}. \tag{8}$$

The expression for the heat decays amplitudes, Eqs. (3), (7) and (8), contain important photophysical parameters such as $(\Phi_{FM})_0$, $(\Phi_{TM})_0$ and q_{PT}, along with τk_{QM}, which also appears in $\Phi_{FM}/(\Phi_{FM})_0$, Eq. (1). The quenching process

looks the same as fluorescence data (see Eq. (1)) regardless of the presence of intersystem crossing, whereas the expressions for the heat release show a remarkably different behaviour depending on the existence of intersystem crossing. This difference opens the possibility of distinguishing between the two mechanisms by means of photoacoustics. It is important to note that the time scale of the slower heat decay is of special interest in the field of protein physical chemistry, since it may give access to slower dynamics like large motions of part of a macromolecule.

3. Materials and methods

All measurements were made at room temperature in air saturated solutions.

3.1. Materials

Bovine serum albumin (BSA), essentially fatty acid free, papain, from Carica Papaia, carbonic anhydrase, KI, Bromocresol green and Fluorescein-5-isothiocyanate (FITC) were obtained from Sigma, St Louis, USA while 6-acryloyl-2-dimethylaminonaphtalene (Acrylodan) was from Molecular Probes, Eugene, OR, USA. All chemicals were used as received with no further purification. The solutions were prepared either in 10 mM Tris-HCl or phosphate buffer. Disposable Sephadex G-25 M columns were model PD-10 from Pharmacia, Uppsala, Sweden.

3.2. Synthesis of the adducts

Stock solutions of FITC in buffer at pH 7.0, or acrylodan in acetonitrile were prepared and added to the protein solution to reach a final molar ratio dye/protein of $\approx 5/1$. Solutions were stirred overnight at 4°C.

The adduct was then purified by means of a disposable Sephadex G-25 M column thorougly rinsed with bidistilled water and equilibrated with buffer for at least 1 hour before application of the sample; two fluorescent bands formed upon elution, the first corresponding to the labelled protein, the second to the free dye and were easily separated.

3.3. Analysis of extent of labelling

Evaluation of labelling efficiency was estimated spectroscopically, and the molar ratio of labelled proteins can be calculated from

$$\text{dye/protein} = \frac{\mathrm{OD}_{493}/\epsilon_{493}(\mathrm{D})}{(\mathrm{OD}_{280} - R \times \mathrm{OD}_{493})/\epsilon_{280}(\mathrm{P})}$$

for FITC, and

$$\text{dye/protein} = \frac{\mathrm{OD}_{360}/\epsilon_{360}(\mathrm{D})}{(\mathrm{OD}_{280} - R \times \mathrm{OD}_{360})/\epsilon_{280}(\mathrm{P})}$$

for acrylodan, where it is assumed that no free dye is present in the fraction. In the previous expression, OD_{493} (OD_{360}) and OD_{280} represent the absorbances of the adducts at 493 (360) and 280 nm respectively, and $\epsilon_{493}(\mathrm{D})$($\epsilon_{360}(\mathrm{D})$) and $\epsilon_{280}(\mathrm{P})$ are the molar extinction coefficients of the free dye and the free protein respectively; the absorbance spectra of the components are supposed to be unaffected by binding. The numerator represents the concentration, in moles per liter, of the dye in the conjugate sample and assumes the absorbance at 493 (360) to be that of the dye only, with no contribution from the protein. The molar extinction coefficient of the protein alone must be known and the ratio R of the absorbances of the free dye at 493 (360) and 280 needs to be measured.

The molar extinction coefficient of FITC is $\epsilon_{493}(\mathrm{D}) = 7.4\ 10^4\ \mathrm{cm}^{-1}\ \mathrm{M}^{-1}$, and for the ratio R a value of 1.55 at pH 7.0 can be calculated. Prendergast et al. [21] report for acrylodan a value of $\epsilon_{360}(\mathrm{D}) = 1.29\ 10^4\ \mathrm{cm}^{-1}\ \mathrm{M}^{-1}$, which gives $R = 0.8$.

The values of $\epsilon_{280}(\mathrm{P})$ are: $5.58 \times 10^4\ \mathrm{cm}^{-1}\ \mathrm{M}^{-1}$ for carbonic anhydrase (MW = 31000), $5.25 \times 10^4\ \mathrm{cm}^{-1}\ \mathrm{M}^{-1}$ for papain (MW = 21000) and $5 \times 10^4\ \mathrm{cm}^{-1}\ \mathrm{M}^{-1}$ for BSA (MW = 63000) [28].

Typical molar ratios FITC/protein for the adducts were 0.89 for carbonic anhydrase, very close to unity for BSA and about 0.1 for papain; lower efficiency was obtained with acrylodan, the fractions being 0.1, 0.4 and 0.1 respectively. This

low efficiency did not allow reliable PA measurements on these adducts, since the absorption of the purified fractions was too low to give a good signal-to-noise ratio. Due to the higher sensitivity of the technique, fluorescence measuremens were still possible. The low extent of labelling obtained for papain was attributed to the fact that the sample was oxidized, with expected lower reactivity at the sulphydryl group of the cysteine in the active site. BSA and carbonic anhydrase were more easily labelled with FITC than with acrylodan and for the latter serious problems of solubility of the adduct arose, whose origin was not investigated.

No tests for enzyme activity were performed after labeling.

3.4. Photoacoustic measurements

In our PA apparatus, photoexcitation is achieved by the output of an excimer-pumped dye laser (Lambda Physik, model EMG50 XeCl excimer laser, FL3100 dye laser, 5 ns pulse width) operated at about 5 Hz repetition rate. The laser dyes used in this study were Coumarin 4800 (peak emission at 480 nm) for FITC and *p*-terphenyl (peak at 343 nm) for acrylodan. The laser pulse is divided by a beam splitter so that about 15 μJ is incident on the sample cuvette, while about 4 μJ is diverted to an energy meter probe (Laser Precision RjP-735). The energy meter (Laser Precision RjP-7620) thus provides a measure of the pulse energy incident on the sample. A 20 cm lens is placed about 15 cm before the front surface of the cuvette. The linearity of the photoacoustic response with pulse energy was checked. The heat deposited by the photoinitiated events is detected by a Panametrics V103, 1 MHz piezoelectric-based transducer, clamped to the side of the cuvette with a layer of silicone grease interfacing transducer and cuvette; an aluminum foil is placed between cuvette and transducer in order to minimize the disturbance coming from the strong fluorescence emitted by the sample. Care is taken in not disturbing the cuvette/transducer arrangement while changing samples. The transducer signal is amplified (Panametrics ultrasonic preamplifier, 60 dB gain, 0.5–5 MHz bandwidth and LeCroy 6103) and digitized by a LeCroy TR8837 32 Ms/s, 8-bit, 100 MHz bandwidth transient recorder. Data from 100 laser pulses are averaged to give one photoacoustic waveform. Data are collected by a PS2/50 IBM personal computer using Catalyst software.

Preprocessing of the experimental data is necessary, since the measured signal must be subtracted of the experimental baseline, and normalized for the incident pulse energy and the solution absorbance at the excitation wavelength. The instrumental transfer function is determined by recording the photoacoustic waveform of a compound that releases the absorbed energy as heat with unit efficiency within a few ns [24].

3.5. Fluorescence measurements

Static fluorescence measurements were performed on a Perkin Elmer LS50 computer interfaced fluorometer. The data were collected with both excitation and emission slits at 2.5 nm, the excitation wavelength being 490 nm for FITC and 343 for acrylodan. Emission spectra were corrected for the solution absorbance at the excitation wavelength and the spectral sensitivity of the detection system.

Time-resolved fluorescence was performed on a home-built single-photon counting apparatus equipped with a nitrogen flash lamp (199F Edimburgh Instruments) pulsed at 20 KHz, a stop photomultiplier (Philips XP2020 Q) and fast NIM electronics (Ortec, Silena, Tennelec). The time resolution was routinely 53 ps per channel and the decays were recorded in a 1024 channel memory. The instrumental response function was automatically collected, in alternation with fluorescence decay, by measuring the scattering of a glycogen solution, and the automatic sampling of data was driven by a microcomputer. The fluorescence intensity decay data were analyzed as a sum of exponentials by means of a nonlinear least squares algorithm.

3.6. Photoacoustic data analysis

The process of photoacoustic waveform deconvolution has already been described in the litera-

ture [15]. Numerical deconvolution of photoacoustic waveforms is performed by means of an iterative nonlinear least-squares algorithm, which provides the fractional amplitudes and the lifetimes of the heat transients. When the lifetime of the transient is shorter than a few ns, the evolved heat is integrated by the transducer and the amplitude of the corresponding decay is usually called prompt heat α [7]. α can also be obtained by the ratio of the amplitudes of the sample and reference waveforms, provided that the sample does not undergo any thermal relaxation in the range 50 ns–5 μs. The heat deposited in times longer than some μs is not sensed by the transducer and may be regarded as "lost" energy.

Quenching data were fitted with the equations introduced in section 2 by means of an iterative nonlinear least-squares algorithm. When possible, the expressions for fluorescence quantum yield ratios and photoacoustic amplitudes were used to simultaneously fit the data coming from static fluorescence and time-resolved photoacoustics [16]. The expression $\Phi_{FM}/(\Phi_{FM})_0$ was assumed to be proportional to the ratio of the fluorescence amplitude with (F) and without (F_0) quencher.

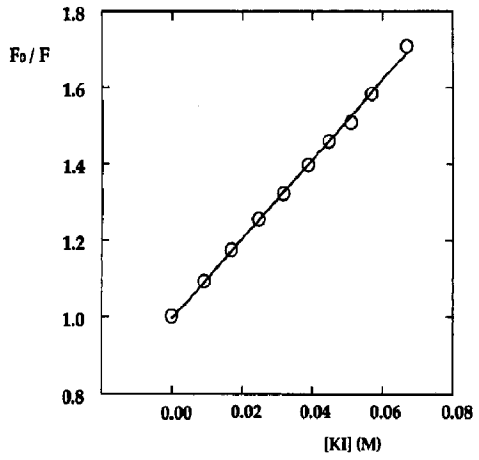

Fig. 1. Stern–Volmer plot for fluorescence quenching of FITC with KI. The quenching constant that has been recovered is $K = 11.1\ M^{-1}$ with sum of squares 0.0001 and correlation coefficient 0.999.

4. Results and discussion

Acrylodan has a fluorescence emission peaked at 472 nm when bound to BSA, whereas papain and carbonic anhydrase adducts have maxima at 496 and 500 nm respectively. These data are indicative of a hydrophobic pocket on each binding site [21], the least polar one being on BSA. Though not unambiguous, this finding reflects the degree of exposure to the solvent the labeling site has. In fact an easier access to the site would reasonably result in a more markedly polar environment, while the apolarity of the sites is suggestive of a shielding from water.

Fluorescence quenching of FITC free in solution with KI, and the Stern–Volmer plot of the fluorescence emission intensity, shown in Fig. 1, is linear with a slope $K = 10.4\ M^{-1}$. Determination of fluorescence lifetime allowed us to estimate the bimolecular quenching constant, k_{QM} from $K = \tau k_{QM}$. The average lifetime in the absence the quencher is 4.1 ns and this gave us a value for k_{QM} of $2.7\ 10^9\ M^{-1}\ s^{-1}$, indicating a diffusion limited process of quenching. The quenching constant has been determined also by studying the average fluorescent lifetime versus KI concentration. The lifetime decreases with increasing [KI], showing that the quenching process is dynamical, and a plot of τ_0/τ versus [KI] (not shown) is linear with the same slope as the one recovered from static fluorescence data. These values are in very good agreement with previously reported fluorescence quenching constants [17].

Numerical deconvolution of PA data evidenced only prompt heat emission for free FITC and the dependence of α on KI concentration is reported in Fig. 2, where the solid line is the result of fitting of Eq. (3) to experimental data. The agreement between theory and experiment is fairly good and extrapolation of the fluorescent quantum yield $(\Phi_{FM})_0$ from quenching data gives essentially the same value obtained from the [KI] = 0 point. Unexpectedly the recovered value for K is $3.3\ M^{-1}$, small if compared to the constant of $10.4\ M^{-1}$ obtained from fluorescence This discrepancy persists in all of the FITC labeled proteins, indicating a systematic disagreement between theory and experiment.

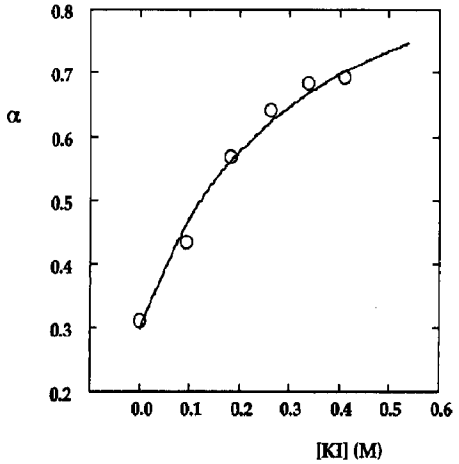

Fig. 2. Photoacoustic quenching by KI of FITC free in solution. α represents the result of a single component decay fitting to experimental data. Typical absorbance was 0.2–0.3 at the excitation wavelength (490 nm); sample and reference (bromocresol green) were equal within 5%; differences in absorbance were accounted for by means of the normalization factor $(1-10^{-A})$ [15]. Solid line is the best fit with Eq. (3), which gave $(\Phi_{FM})_0 = 0.76$ and $K = 3.3\ M^{-1}$, sum of squares 0.004 and correlation coefficient $R = 0.97$.

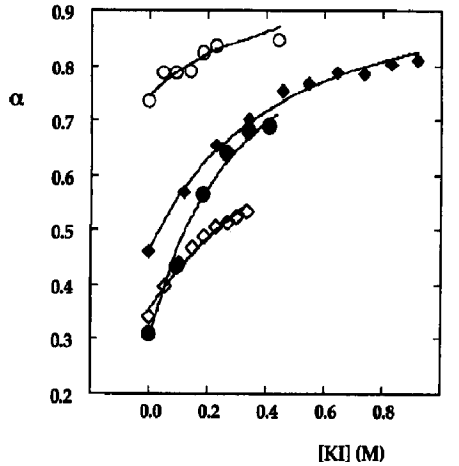

Fig. 3. Photoacoustic amplitudes (single decay data analysis) for the different samples studied: solid lines in the plot F versus [KI] are the best fit of Eq. (3). (●) free FITC, (○) BSA-FITC; (♦) carbonic anhydrase-FITC; (◇) papain-FITC.

Fig. 3 reports the dependence of α on KI concentration for each of the three proteic adducts, the solid lines being the result of the fitting of Eq. (3) to the experimental data. Only prompt heat was detected in each case. The difference in the fluorescence quantum yields (y intercepts) and quenching constants (slopes) of the different samples is evident from the plots. The parameters resulting from fitting are reported in Table 2.

Fluorescence quenching constants of the different samples show that the quenching process is slightly more efficient for carbonic anhydrase-FITC than for papain-FITC, and in both cases the value of K is smaller than the one determined for free FITC, in accordance with a certain degree of shielding from the solvent, as suggested above.

In order to remove the discrepancy between the quenching constants from fluorescence and PA, the possibility has been investigated that the photophysics of FITC is better described by a model where the intersystem crossing to a triplet state is considered.

Fluorescein and some of its fluorescent derivatives undergo intersystem crossing to a triplet state [29,30] with a very different efficiency, ranging from 0.05 ± 0.02 for unmodified fluorescein,

Table 2
Fluorescence quenching by KI of FITC and of its complexes with the proteins considered in this study: results from fluorescence (F) and photoacoustics (PA). Fluorescence data were analyzed with the Stern–Volmer equation, Eq. (1), while photoacoustics data with the simple fluorophore model, Eq. (3). The table reports the fluorescence lifetimes τ as determined by single-photon counting, which were used to determine the bimolecular quenching constant k_{QM}. All of the measurements were carried out with excitation at 490 nm, corresponding to a molar energy content of 58.37 kcal/mol

Sample	F			PA		
	$K\ (M^{-1})$	τ (ns)	$k_{QM}\ (M^{-1}\ s^{-1})$	$(\Phi_{FM})_0$	$k_{QM}\ (M^{-1}\ s^{-1})$	$K\ (M^{-1})$
free FITC	10.40	4.1	2.5×10^9	0.76	0.8×10^9	3.3
FITC-carbonic anhydrase	4.90	3.9	1.3×10^9	0.57	0.6×10^9	2.2
FITC-papain	4.24	3.9	1.1×10^9	0.68	0.3×10^9	1.3
FITC-BSA	5.81	3.8	1.5×10^9	0.26	0.5×10^9	1.8

to 0.49 ± 0.07 for eosin, to 0.71 ± 0.1 for dibromefluorescein, up to 1.07 ± 0.13 for erytrosin. FITC itself is known to undergo intersystem crossing to a triplet state [31] with a rather low efficiency (0.05) and a fairly long lifetime, falling outside our instrumental sensitivity. Depending on the substituent, the rate of intersystem crossing may be strongly enhanced with respect to the unsubstituted fluorescein. FITC and its thiol adducts may therefore reflect a mechanism that is similar to the one observed in fluorescein derivatives, i.e. the intersystem crossing probability may be altered to a different extent upon binding to different protein environments. Support to this idea comes from the recent work of Indig et al. [32], who demonstrated the involvment of the triplet state of malachite green, a nonfluorescent fluorescein derivative, in the nonradiative deexcitation of its singlet excited state. Free malachite green shows emission of prompt heat with unit efficiency, whereas upon covalently binding to a protein, the chromophore shows a nonradiative efficiency lower than one. After a careful analysis of the photophysics of the system, they concluded that the intersystem crossing to the triplet state was responsible of the lowering of prompt heat emission.

Based on this ideas, PA data of fluorescence quenching were analyzed in the frame of the model developed for an enhanced intersystem crossing probability, and the results are reported in Table 3. Due to the higher number of fitting parameters present in these equations and to the large errors on experimental data, Eq. (7) was rearranged in order to have only three variable parameters. The equation for α_1 was rearranged in the following way:

$$\alpha_1 = \frac{A_1 + A_2 K[Q]}{1 + K[Q]} \tag{9}$$

where A_1 and A_2 have the following meaning:

$$A_1 = 1 - (\Phi_{FM})_0 \frac{\lambda_{ex}}{\lambda_{em}} - (\Phi_{TM})_0 \frac{E_T}{E},$$

$$A_2 = 1 - \frac{E_T}{E}. \tag{10}$$

Table 3
Fluorescence quenching of FITC by KI: results from the analysis of PA data in the frame of the triplet state model. The only sample for which it was possible to determine $(\Phi_{TM})_0$ was the free FITC; for the other samples 0.15 and 0.77 were assumed as the limits of this parameter, and $(\Phi_{FM})_0$ was accordingly calculated

Sample	K (M^{-1})	$(\Phi_{TM})_0$	E_T/E	$(\Phi_{FM})_0$
free FITC	10.2	0.15	0.5	0.70
FITC-carbonic anhydrase	5.8	–	0.55	0.55–0.9
FITC-papain	4.2	–	0.33	0.43–0.66
FITC-BSA	5.7	–	0.3	0.2–0.3

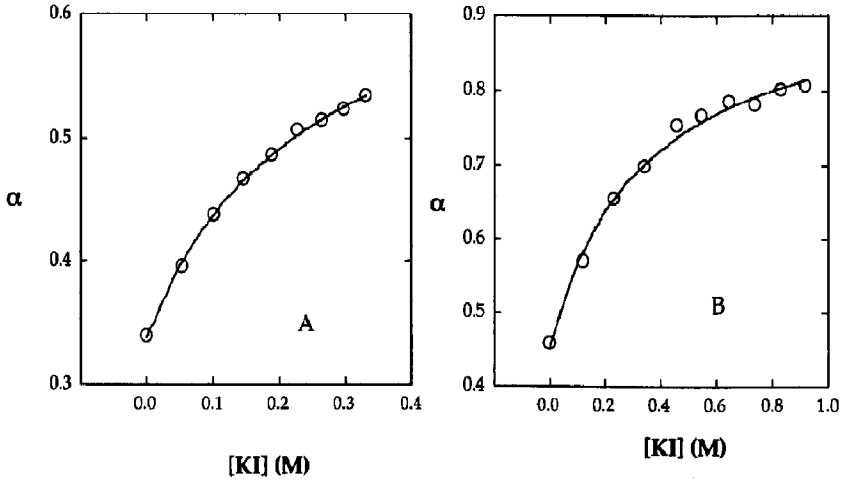

Fig. 4. Fitting of photoacoustic amplitudes (single decay data analysis) by means of Eq. (5) for the FITC-papain (A) and FITC-carbonic anhydrase (B) adducts.

From A_2 it was easy to obtain E_T whereas extracting either $(\Phi_{FM})_0$ or $(\Phi_{TM})_0$ from A_1 requires the knowledge of the other parameter. The numerical results of the fitting are shown in Table 3. Visual inspection of the fitting curves, as well as the sum of the squares of the residuals, show a significant improvement, and a good accordance between the quenching constants is now obtained for both free FITC and the protein bound forms. In Fig. 4 we report for comparison the results of the fitting with Eq. (7) for the data from the adducts FITC-papain and FITC-carbonic anhydrase. Knowing $(\Phi_{FM})_0$ from literature data, the value of $(\Phi_{TM})_0$ of free FITC can be estimated as 0.15, approximately three times larger than the value reported in the literature. Using 0.15 and 0.77 as limiting values for $(\Phi_{TM})_0$, an estimate of $(\Phi_{FM})_0$ can be obtained for each of the samples. A comment is needed about the value of E_T recovered from the fitting procedure: the values obtained, around 0.5–0.3 E, are low if compared to the values reported for the triplet energy of fluorescein and some of its derivatives [33]. The solutions were not deoxygenated and a possible transfer of the triplet energy to molecular oxygen to form singlet oxygen $O_2(^1\Delta_g)$ can result in a further step in the energy migration pathway, that was not included in the models previously outlined. This would alter the energy content of the fraction of prompt heat by the addition of the further contribution, due to the difference in energy between the triplet and the singlet times the efficiency of this last process. Taking into account this further deexcitation pathway implies a different mathematical treatment of the data, which was not attempted in this work.

In the bound forms, the fluorescence quantum yield of FITC is different from the one FITC has, when free in solution at neutral pH. As stated above, this may reflect in some way the local pH at the binding site of the dye, but, more generally, the observed difference is an indication of the extent of the perturbation to the electronic energy levels of FITC induced by the protein host. A more detailed knowledge of the triplet energy and intersystem crossing quantum yield for each adduct would allow a more precise determination of the fluorescent quantum yield.

The efficiency of labelling with acrylodan was high enough to allow the fluorescence measurements, but too low to perform PA quenching measurements. In Table 4 the results of this quenching study are summarized, which confirm a shielding from the solvent of the environments in which the probe is in the different proteins.

5. Conclusions

Photoacoustic and fluorescence data of extrinsic fluorophores are informative of the local structure and dynamics of the binding site. Due to the limited sensitivity and accuracy of the technique, PA data are affected by larger errors than fluorescence data and the analysis is consequently more uncertain. However, the gain in the quality of the information extracted from the

Table 4
Fluorescence quenching by KI of acrylodan and its complexes with the proteins used in this work. Due to the low efficiency of labelling, PA data are not reported because of sensitivity problems. Nonlinearity in the Stern–Volmer plots was found that was attributed to heterogeneity in the emission; the data were accordingly analyzed [4] to get the quenching parameters. Me-acrylodan is the symbol for the mercaptoethanol adduct of acrylodan, a brightly fluorescent molecule that simulates the binding to the thiol group of the protein [21]

Sample	Solvent	K_1 (M^{-1})	K_2 (M^{-1})	ϕ_1	ϕ_2	τ_2 (ns) [21]	k_{QM} ($M^{-1}\,s^{-1}$)
acrylodan	buffer pH 7.0	23.4	0.5	0.15	0.85	–	–
Me-acrylodan	buffer pH 7.0	12.1	≈ 0	0.64	0.36	1.28	9.45×10^9
A-papain	buffer pH 7.0	12.8	≈ 0	0.36	0.64	4.07	3.14×10^9
A-carbonic anhydrase	buffer pH 7.0	2.23	0.2	0.78	0.22	3.19	0.7×10^9
A-BSA	buffer pH 7.0	10.6	≈ 0	0.38	0.62	–	–

quenching process is evident from the previously discussed experiments. The access to long-lived states, as the triplet state, make available a further sorce of dynamical information, in the same way as the T_1–S_0 phosphorescence decay is a very useful probe of large (and slow) movements of the macromolecule. The study of the dependence of these processes on other important photophysical parameters, such as temperature and viscosity, will help to distinguish different sources of photoacoustic signal, since in this way a volumetric contribution from some light-induced conformational change of the adducts would become evident [34]. Finally, improvements in data acquisition and analysis could reduce the experimental errors and increase the sensitivity, and eventually give access to more accurate estimates of the photophysical parameters.

Acknowledgments

The author wishes to acknowledge Professor J.R. Small of Eastern Washington University for initial discussion on the project and for supplying the nonlinear least-squares fitting program. Thanks go to Professor P.R. Crippa as well, who took me in touch with photoacoustics and encouraged constantly my work. Finally the author wishes to thank G. Campani for his work on software development and implementation of data preprocessing routines and Dr. L. Brancaleon for his collaboration and friendship. This work was supported by the Italian Ministero per l'Università e per la Ricerca Scientifica e Tecnologia (MURST) and the Consiglio Nazionale delle Ricerche (CNR).

References

[1] R.P. Haugland, Handbook of fluorescent probes and research chemicals, (Molecular Probes, 1989).
[2] M.R. Eftink, in: Time-resolved laser spectroscopy in biochemistry, ed. J.R. Lakowicz, Vol. 1204 (SPIE–The International Society for Optical Engineering, Bellingham, WA, 1990) p. 406.
[3] M.R. Eftink and K.A. Hagaman, Biophys. Chem. 25 (1986) 277.
[4] M.R. Eftink and C.A. Ghiron, Anal. Biochem. 114 (1981) 199.
[5] J. Duszynski, A. Dupuis, B. Lux and P.V. Vignais, Biochem. 27 (1988) 6289.
[6] D.A. Johnson and J. Yguerabide, Biophys. J. 48 (1985) 949.
[7] S.E. Braslavsky and G.E. Heibel, Chem. Rev. 92 (1992) 1381.
[8] W. Lahmann and H.J. Ludewig, Chem. Phys. Letters 45 (1977) 177.
[9] J.R. Small, J.J. Hutchings and E.W. Small, in: Fluorescence detection III, ed. E.R. Menzel, Vol. 1054 (SPIE–The International Society for Optical Engineering, Bellingham, WA, 1989) p. 26.
[10] J.R. Small and S.L. Larson, in: Time-resolved laser spectroscopy in Biochemistry II, ed. J.R. Lakowicz, Vol. 1204 (SPIE–The International Society for Optical Engineering, Bellingham, WA, 1990) p. 126.
[11] J.E. Sabol and M.G. Rockley, J. Photochem. Photobiol. A 40 (1987) 245.
[12] K. Heihoff and S.E. Braslavsky, Chem. Phys. Letters 131 (1986) 183.
[13] T.Q. Ni and L.A. Melton, J. Photochem. Photobiol. A 67 (1992) 167.
[14] J.R. Small, S.H. Watkins, B.J. Marks and E.W. Small, in: Time-resolved laser spectroscopy in biochemistry II, ed. J.R. Lakowicz, Vol. 1204 (SPIE–The International Society for Optical Engineering, Bellingham, WA, 1990) p. 231.
[15] J.R. Small, L.J. Libertini and E.W. Small, Biophys. Chem. 42 (1992) 24.
[16] C. Viappiani and J.R. Small, in: Time-resolved laser spectroscopy in Biochemistry III, ed. J.R. Lakowicz, Vol. 1064 (SPIE–The Society of Photo-optical Instrumentation Engineers, Bellingham, WA, 1992) p. 285.
[17] D.A. Johnson and J. Yguerabide, Biophys. J. 48 (1985) 949.
[18] R. Bernhardt, N.T.N. Dao, H. Stiel, W. Schwarze, J. Friedrich, G.R. Janig and K. Ruckpaul, Biochim. Biophys. Acta 745 (1983) 140.
[19] M.J. Geisow, Exp. Cell Res. 150 (1984) 29.
[20] V.N. Hingorani and Y.K. Ho, Biochem. 26 (1987) 1633.
[21] F.G. Prendergast, M. Meyer, G.L. Carlson, S. Iida and J.D. Potter, J. Biol. Chem. 258 (1983) 7541.
[22] G. Weber and F.G. Farris, Biochem. 18 (1979) 3075.
[23] T.J. Peters, in: Advances in protein chemistry, Vol. 37 (Academic Press, Inc., 1985) p. 161.
[24] J.E. Rudzki, J.L. Goodman and K.S. Peters, J. Am. Chem. Soc. 107 (1985) 7849.
[25] O. Stern and M. Volmer, Physik. Z. 20 (1919) 183.
[26] J.R. Lakowicz, Principles of fluorescence spectroscopy, (Plenum Press, New York, 1983) p. 496.
[27] J.B. Birks, Photophysics of aromatic molecules, (Wiley-Interscience, New York, 1970) p. 704.
[28] Worthington, Enzymes, enzyme reagents and related biochemicals, (Worthington Biochemical Corporation, Freehold, NJ, 1972).

[29] P.G. Bowers and G. Porter, Proc. Roy. Soc. A 299 (1967) 348.
[30] A. Chartier, J. Georges and J.M. Mermet, Chem. Phys. Letters 171 (1990) 347.
[31] A.F. Corin, E. Blatt and T.M. Jovin, Biochem. 26 (1987) 2207.
[32] G.L. Indig, D.G. Jay and J.J. Grabowski, Biophys. J. 61 (1992).
[33] I. Carmichael and G.L. Hug, in: CRC Handbook of Organic Photochemistry, ed. J.C. Scaiano, Vol. I (CRC Press, Boca Raton, FL, 1989) p. 369.
[34] K.S. Peters, T. Watson and K. Marr, Ann. Rev. Biophys. and Biophys. Chem. 20 (1991) 343.